Two Dimensional Numerical Analysis of Tunnel by the Finite Element Method: Evaluation Case of "Djelfa, Algeria"

TALEB Hosni Abderrahmane [*1,2], **CHERIET Fayssal** [3,4], [3,]**AZZOUZI Oumelkhir,**
[3]**LEDJDEL Hanane Chaima.**

[1]*FIMAS Laboratory, University of Bechar – ALGERIA.*
[2]*Department of Civil Engineering and Hydraulic, Institute of Science and Technology, University Center of Mila. ALGERIA.*
[3]*Civil Engineering Department, University of Djelfa, 17000 Djelfa, ALGERIA.*
[4]*Laboratory Environment, Water, Geomechanics and Buildings (LEEGO), ALGERIA*

[*1,2] talebhosni@yahoo.fr

Abstract

Tunnels were required in building zones as a result of the growth and expansion of large cities. Tunnels are an important component of today's construction area. They are significant in terms of infrastructure and economy. Djelfa tunnel with a length of 800 m was excavated based on the geotechnical, geological, and geometrical requirements of the region. The tunnel is modeled in this study. The settlement caused by excavation is calculated using the numerical finite element methods (OptumG2). According to the numerical modeling of this research, the results show that the value of a settlement, in this case, are agree with the safety and stability of the Djelfa Tunnel.

Keywords: Djelfa; Tunnel; Stability; Finite Element Method; OPTUMEG2.

1. Introduction

The population of Djelfa has augmented in recent years. According to census data, the population increased to 1.223.223 persons in 2020 [1]. This rapid population growth necessitates the construction of new towns and urban areas, as well as the development of transportation systems such as bridges, roads, and underground transportation systems such as tunnels, which have become an integral part of metro cities and play an important role in a country's development. These structures have become a key feature of metro cities because they are an efficient means of utilizing space. The tunnels have been significant in lowering travel time and boosting a country's defense and transport systems. They link the majority of naturally isolated regions separated by natural obstacles such as mountains.

The tunneling may be separated into three phases. To begin, there is planning (feasibility study), which identifies the project's limitations and dangers, as well as sketching and providing a draft design for the tunnel; Second, engineering, which is concerned with creating exact and constructible designs; Finally, the

tunnel's pre-construction design, as well as the maintenance plan, will be built, executed, and updated [2]. The Designers encounter a variety of obstacles, mostly associated with: The security of workers during construction activities; the excavation-provoked settlements; the face and the cavity must be stable, as well as the end product's quality; the viability of the building process is thus heavily influenced by the unfavorable hydrological geological, or geotechnical behavior of excavated mass (soils and rock), [3]. The building of this type of structure frequently confronts stability issues. As a result, their designs are now based on in-depth geotechnical investigations and risk analyses to assure the structures' and users' safety [4]. Rock tunnels are common and have been the subject of research for a long time [5–9]. Because of better computer efficiency, the numerical technique is commonly used to analyze tunneling problems for various loading types [10-13]. And the numerical technique is frequently utilized to research tunnel complexity behavior [14–18].

In this paper, the tunnel of Djelfa is modeled by using the numerical finite element methods. The settlement caused by excavation is calculated with the OptumG2 program. The shape of a tunnel, such as a circular, rectangular, or arch, has an impact on its behavior. Analytical, physical, and numerical model approaches were used to study many shapes of tunnels [19–22]. For that, we analyze the tunnel of Djelfa with a D shape, see figure 3.
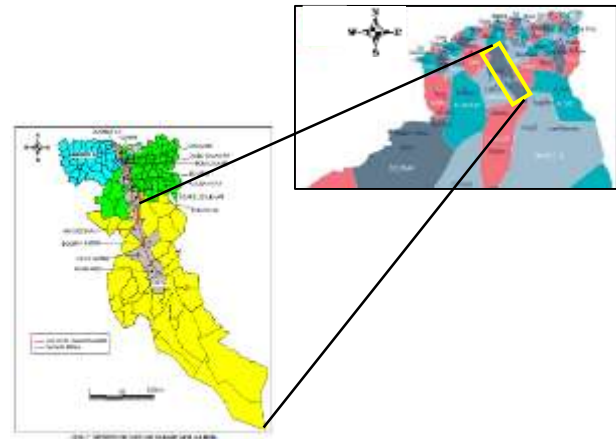
Figure 1. Djelfa tunnel location map

2.   Description of the study site

In the project context construction of the newly electrified line between Boumedfaa and Djelfa (280 KM, red line) see figure 1, the purpose of this part of our research is to model and analysis the tunnel.

2.1. Location of Djelfa

Due to its strategic location (figure 1), it connects the north, with the south, and the east with the west. Djelfa, This state is considered a link between 9 states. 300 km south of the capital (Algiers), and occupies an area of 32, 256, 35 km2, representing 1.36% of the total area of the country (Algeria). It is border 9 states, Medea and Tissemsilt to the north, Ouargla, Ghardaia, and El Oued to the south, Biskra and M'sila toward the east, and the provinces of Laghouat and Tiaret to the west. See figure 1 (yellow rectangular color).

2.2.General Geological Framework

The geological and geotechnical characteristics of the tunnel crossed by the area of the layout of the road are described in figure 2.
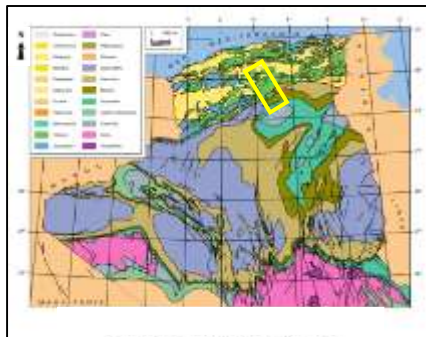
Figure 2. Geological map of Algeria

The study area is located, geologically, around the Alpine Algeria, surrounded by the Complex region structurally of the Tellian Nappes and the Atlas Fold, browsing approximately, from North to South, the Tellian Atlas, the High Plateaus, and the northern foothills of the Saharian Atlas, and ending near the Djebel Senalba massif. Figure 2 shows the geological sector where the study area is located [23].

Figure 3. Tunnel excavation (a), lining concrete (b)
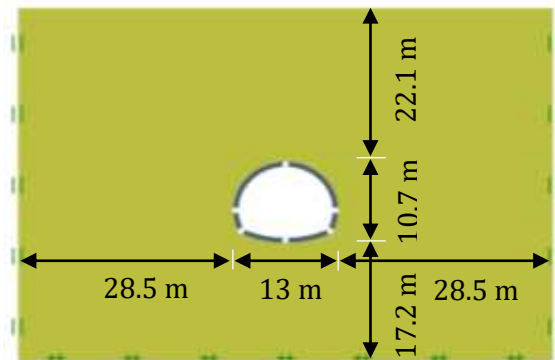
Figure 5. Geometry of the tunnel
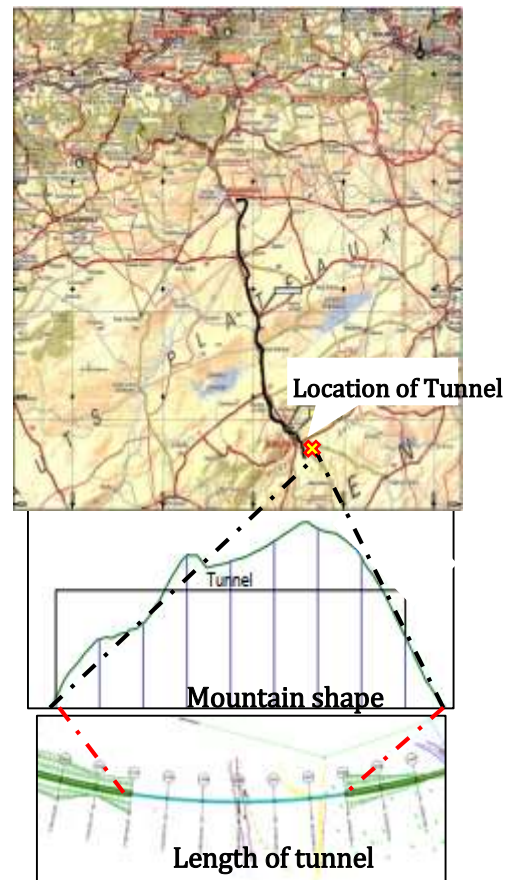
Figure 4. Djelfa mountain, length tunnel , and location map

Figure 4 shows the shape of the mountain, the length of the tunnel, and its location on the map. The tunnel object of this study is projected

between PPKK 227+200 and 227+800, and it has a length of 600 m. Figure 3, illustrates the beginnings of tunnel excavation (a) and lining concrete work (b).

3. Numerical Study

OPTUMG2 [24], finite element software was used to apply the 2D plane strain analysis with the Mohr-Coulomb criteria to represent the elastoplastic model of soil (one layer) in this study. The geometry of the model is shown in figure 5. The width and height of the total modeling domain are 70 m and 50 m, respectively. The tunnel has a 22.1 depth of overburden. The base of the boundary condition is fixed see figure 5. In addition, the lining concrete thickness was 0.25 m. The parameters of the model are shown in Table 1.

3.1. Modeling phases

There are three parts (steps) to the modeling in this study: we start with the calculation of the initial stress state, in this step condition takes into consideration the impact of vertical stress on the depth gradient under gravity's influence. In the second phase, the tunnel is excavated. With a relaxation ratio of 0.3, the tunnel perimeter (wall) is given a relaxation ratio that allows for a proportional reduction in the pressures on the excavations totally supported in this step. In the last step, the tunnel boundary support (concrete lining) was erected. The purpose of this phase is to maintain the safety of the tunnel.

4. Resultants And Discussion

In this numerical section, we want to examine the vertical and horizontal displacements at the ground surface level (Y = 50 m) and near the tunnel at 28 m and 17.1 m. As shown in figure 6. The study was

carried out in the same way for each of the Y heights (50 m; 28 m; 17.5 m).
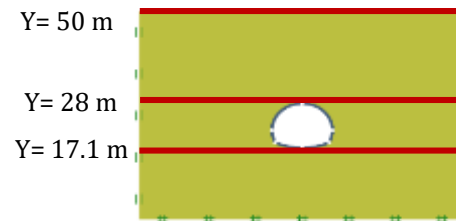
Figure 6. The tunnel's transverse section.

Table 1 shows the geotechnical properties of soil and concrete lining modeling features used in this case.

Table 1. The properties of the soil, and concert lining

SOIL PROPERTIES	Value
Young's module E (MPa)	4.026 E+04
Poisson's ratio ϑ	0.27
Friction angle φ (°)	47
Cohesion c (KPa)	190
Saturated density γ_{sat} (KN/m^3)	24
CONCRETE LINING	
Thickness (cm)	25
Weight W (kg/m/m)	625
Section area A (cm2/m)	2500
Moment of inertia I (cm4/m)	1.302 * 105
Plastic section modules S (cm3/m)	1.563 * 104
Young's module E (MPa)	2.54 * 104
Yield strength	28

4.1. Vertical and horizontal displacements

As a result, the design engineer should give consideration to the details of the project. The goal of this research is to quantify vertical and horizontal displacements using the stated profiles of Y = 50, 28 m, and 17.1 m.
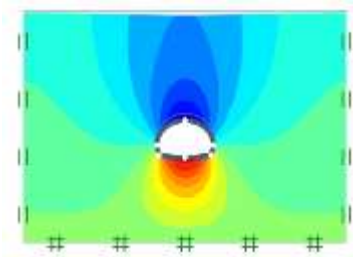
Figure 7. Deformation of soil and concrete lining

The deformation at the lining contact and the soil mass was examined as part of the stability investigation of the tunnel. Figure 7 illustrates that the deformations are more developed at the top of the tunnel than they are at the bottom. The displacements are represented on a color scale for the unit meter. The distribution of the soil displacements caused by tunnel excavation.
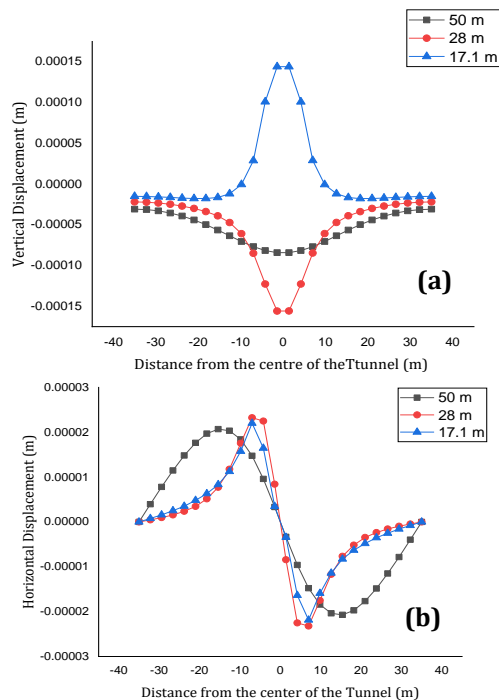
Figure 8. Vertical (a), and Horizontal displacement (b)

The idea is to measure the vertical and horizontal displacements while using the Y = 50, 28 m, and Y=17.1 m profiles. Figure 8 (a) shows the tunnel's final surface settling curves (Y =50 and 28 m) after excavation, with the greatest surface settlement value being 1.5E-4 m above the tunnel (Y=28 m). The settlement is 0.75E-4 m at the ground surface level Y=50 m, however the displacement soil under the tunnel (Y=17.1 m) has the same results as the ground surface level, 0.75E-4 m, but in the opposite direction of the tunnel void (the vertical direction).

Figure 8 (b), shows the horizontal displacements, they will grow near the tunnel's center, with minor displacements on the sides. The maximum horizontal displacement amount occurred at the sides of the center of the profile tunnel (Y=28 and 17.1 m) with a value of $\pm$ 0.25E-4 m. the smallest displacements at the ground surface level (Y=50 m) with a value of 0.2E-4 m.
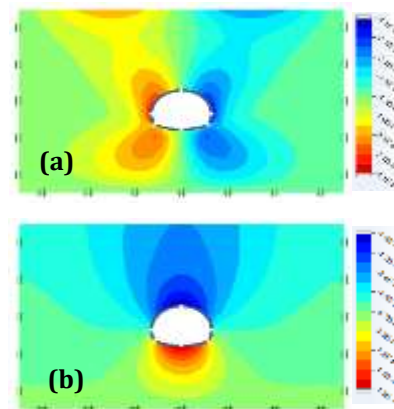
Figure 9. Displacements (m): Horizontal (a), and Vertical (b).

The horizontal displacement of soil (4.1E-5 m), is lower than the vertical displacement of soil (1.5E-4 m). The horizontal displacements were likewise found to be symmetrical in relation to the tunnel's vertical axis (figure 9 a). The highest horizontal displacements occur on the free surface, on both the left and right sides of the

tunnel. Figure 9 (a), illustrates that the left side of the tunnel has positive displacements (a shade of red color), while the right side has negative displacements. They correspond to a tendency for horizontal convergence of the ground towards the center of the tunnel.
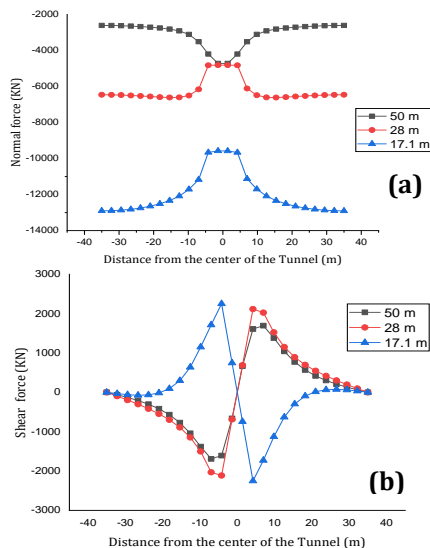
Figure 10. Normal (a), and Shear force (b)

The normal forces of the three profiles present in figure 10 (a), we notice that the normal force at the ground surface level (Y=50 m) decreases at the center of the profile tunnel with a value of 4400 KN. The normal force increases in harmonization in both levels (Y=28 and 17.1 m). The shape of the normal force caused by tunnel excavation. It is observed that the normal forces are found to be symmetrical in relation to the tunnel's vertical axis.

As shown in figure 10 (b), the shear force grow near the tunnel's center. The maximum shear force amount occurred at the sides of the center of the profile tunnel (Y=28 and 17.1 m) with a value of ± 2100 KN. the smallest shear force at the ground surface level (Y=50 m) with value of 1800 KN. The shear force increases in

harmonization in both levels (Y=50 and 28 m), and the other level (Y=17.1 m) against the previous two levels
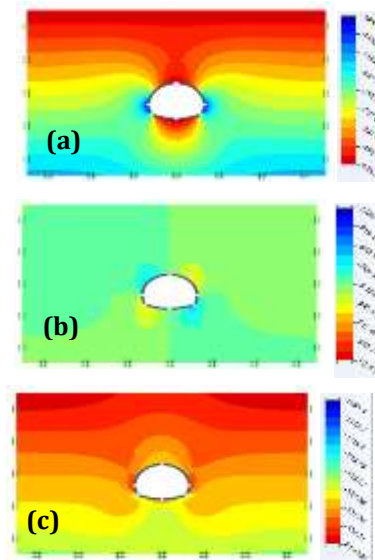
Figure 11. Vertical stress (KPa) (a), Shear stress (KPa) (b), and Horizontal stress (KPa) (c).

The vertical stresses are negative, with a maximum value of -1600.8 KPa, which corresponds to compressions. At the tunnel's left and right lining concrete, the vertical stress concentration is more or less fully developed. As seen in figure 11 (a), the vertical stress distribution is symmetrical with respect to the tunnel's vertical axis. Figure 11 (b) shows the evolution of stress contours for the tunnel following the lining concrete phase, which has maximum concentration stresses of 1225.09 KPa to the right and left of the lining tunnel.

The horizontal stresses on the right and left concrete lining of the tunnel are a minimum of 61.42 KPa. The horizontal stresses at the top and at below the concrete lining of the tunnel are greater than the left and right side stresses. Figure 11 (c) shows that the horizontal stress

distribution is almost symmetrical with respect to the vertical axis of the tunnel.

Figure 12, shows how to view the deformation at the tunnel's perimeter more clearly. Due to soil pressure, deformations in the lining occur, and the development of surface settlement may suggest the creation of a failure zone surrounding the tunnel.

(a)   **(b)**
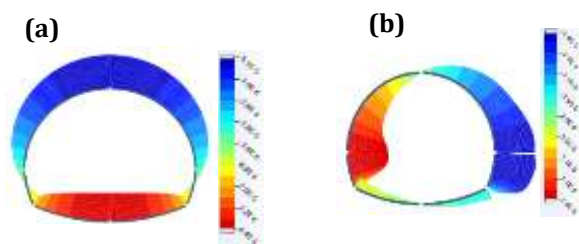
Figure 12. Concrete lining displacements (m): Vertical (a), and Horizontal (b)

The horizontal displacements on both sides of the structure's concrete lining are the same at 1.4E-5 m. On the other hand, the vertical displacements are different. The maximum displacement (-5.1E-5 m) occurs at the top of the tunnel, while the minimum displacement occurs at the tunnel's bottom (4.4E-5 m).

5.   Conclusion

Underground buildings and tunnels are the most structures affected by settlements due to the excavation of rock mass. The study's main goal is to determine the Djelfa tunnel's behavior. First of all the tunnel is stable and safe from the resultants. The numerical results clearly show that when digging in the soil, there is a possibility of settling the ground at the top and swelling at the bottom of the tunnel. The tunnel's top and bottom have the highest displacements. We also note that when it comes to horizontal displacements, are more important on both sides

of the concrete lining at the tunnel level. Vertical displacements are more essential than horizontal displacements. The OptumG2 program is suited for tunnel calculations.

References

[1] https://www.populationdata.net/pays/algerie/.2022.

[2] C. di Prisco, L. Flessati, D. Peila, E.M. Pizzarotti. Book "Handbook on Tunnels and Underground Works" Chapter "Risk management in tunnelling". 1st Edition, 2022, CRC Press, ISBN 9781003256175

[3] C. di Prisco, D. Peila, A. Pigorini. "Handbook on Tunnels and Underground Works" Chapter "Introduction". 1st Edition, 2022, CRC Press, ISBN 9781003256175.

[4] Idris J. Accidents geotechniques des tunnels et des ouvrages souterrains-Methodes analytiques pour le retour d'experience et la modelisation numerique. Doctoral dissertation, Institut National Polytechnique de Lorraine, France. 2007.

[5] Naqvi, M.W., Akhtar, M.F., Zaid, M., Sadique, M.R.: Effect of superstructure on the stability of underground tunnels. Transp. Infrastruct. Geotech. 8, 142–161. 2021. ttps://doi.org/10.1007/s40515-020-00119-6

[6] Zaid, M., Rehan Sadique, M.: A simple approximate simulation using Coupled EulerianLagrangian (CEL) Simulation in Investigating Effects of Internal Blast in Rock Tunnel. Indian Geotech J. 2021. https://doi.org/10.1007/s40098-021-00511-0

[7] Zaid, M., Sadique, M.R., Alam, M.M.: Blast analysis of tunnels in Manhattan-Schist and Quartz-Schist using coupled-Eulerian–Lagrangian method. Innov. Infrastruct. Solut. 6, 69. 2021. https://doi.org/10.1007/s41062-020-00446-0

[8] Zaid, M., Mishra, S.: Numerical Analysis of Shallow Tunnels Under Static Loading: A Finite Element Approach. Geotech Geol Eng. 2021. https://doi.org/10.1007/s10706-020-01647-1

[9] Zaid, M., Sadique, M.R., Samanta, M.: Effect of unconfined compressive strength of rock on dynamic response of shallow unlined tunnel. SN Appl. Sci. 2, 2131. 2020. https://doi.org/10.1007/s42452-020-03876-8

[10] Mroueh, H., & Shahrour, I. 2003. A full 3-D finite element analysis of tunneling adjacent structures interaction. Computers and Geotechnics, 30(3), 245-253.

[11] Pakbaz, M. C., & Yareevand, A. 2005. 2-D analysis of circular tunnel against earthquake loading. Tunnelling and Underground Space Technology, 20(5), 411-417.

[12] Shahin, H. M., Nakai, T., Zhang, F., Kikumoto, M., & Nakahara, E. 2011. Behavior of ground and response of existing foundation due to tunneling. Soils and foundations, 51(3), pp. 395-409.

[13] Zaid, M., Irfan, S., Farooqi, M.A. 2019. Effect of Cover Depth in Unlined Himalayan Tunnel: A Finite Element Approach. In the proceeding of 8th Indian Rock Conference, Indian International Centre, New Delhi, India, 03-04 March 2019, ISBN No. 81-86501-27-1.

[14] Zaid, M., Sadique, M.R.: Blast resistant behaviour of tunnels in sedimentary rocks. International Journal of Protective Structures. 2020. https://doi.org/10.1177/2041419620951211

[15] Zaid, M., Sadique, M.R.: The response of rock tunnel when subjected to blast loading: Finite,element analysis. Engineering Reports. 3:e12293. 2021. https://doi.org/10.1002/eng2.12293

[16] Zaid, M., Sadique, M.R.: Dynamic Analysis of Tunnels in Western Ghats of Indian Peninsula: Effect of Shape and Weathering. In: Pathak K.K., Bandara J.M.S.J., Agrawal R. (eds) Recent Trends in Civil Engineering. Lecture Notes in Civil Engineering, vol 77. Springer, Singapore. 2021. https://doi.org/10.1007/978-981-15-5195-6_57

[17] Zaid, M., Sadique, M.R.: Numerical modeling of internal blast loading on a rock tunnel. Advances in Computational Design, 5(4), 417–443. 2020. https://doi.org/10.12989/ACD. 2020.5.4.417

[18] Zaid, M., Sadique, M.R., Alam, M.M., Samanta, M.: Effect of shear zone on dynamic behavior of rock tunnel constructed in highly weathered granite. Geomechanics and Engineering, 23(3), 245–259. 2020. https://doi.org/10.12989/GAE.2020.23.3.245

[19] Manuello, A., Niccolini, G., Carpinteri, A.: Ae monitoring of a concrete arch road tunnel: damage evolution and localization. Eng. Fract. Mech. 2018. https://doi.org/10.1016/j.engfra cmech.2018.07.029

[20] Amouzandeh, A., Zeiml, M., Lackner, R.: Real-scale CFD simulations of fire in single and double-track railway tunnels of arched and rectangular shape under different ventilation conditions. Eng. Struct. 1–14. 2014. https://doi.org/10.1016/j.engstruct.2014.05.027

[21] Dancygier, A.N., Karinski, Y.S., Chacha, A.: A model to assess the response of an arched roof of a lined tunnel. Tunn. Undergr. Sp. Technol. 56, 211–225. 2016.

[22] Masson, E., et al.: Radio wave propagation in arch-shaped tunnels: measurements and simulations by asymptotic methods. Comptes Rendus Phys. 11, 44–53. 2010.

[23] A Fares, M Rollet, and P Broquet. Méthodologie de la cartographie des risques naturels liés aux mouvements de terrain. Revue française de géotechnique, 69 :63–72, 1994.

[24] Krabbenhoft, K., Lyamin, A., & Krabbenhoft, J. 2016. Optum computational engineering (OptumG2). Computer software]. Retrieved from https://www. optumce.com.